

# Printed UWB Rhombus Shaped Antenna for GPR Applications

A. Chaabane<sup>\*(C.A.)</sup> and M. Guerroui\*

**Abstract:** A new design of a Coplanar Waveguide-Fed (CPW) Ultra Wideband (UWB) Rhombus-shaped antenna for Ground Penetrating Radar (GPR) applications is designed and discussed in this work. The antenna has a simple design which is composed by a rhombus-shaped patch and a modified ground plane. The working bandwidth is improved by removing the metal from the upper part of the ground plane surrounding the patch and by introducing a corrugation geometry in the ground plane. The proposed antenna was designed on a low-cost FR4-substrate having a compact size of  $0.2721\lambda_0 \times 0.2093\lambda_0 \times 0.0157\lambda_0$  at 3.14 GHz. All the simulations were carried out by using the commercially software CST Microwave Studio<sup>TM</sup>. The simulated results show that the designed antenna covers an UWB extending from 3.14 GHz to 13.82 GHz (125.94%) and indicate excellent radiation performances throughout the operating bandwidth. The measured bandwidth is nearly extending between 3.95 GHz and 13.92 GHz (111.58%). Besides, the antenna bandwidth response was checked in close proximity to a mass of Concrete. The obtained results are satisfactory and assure the efficiency of the designed antenna to work as a GPR antenna.

**Keywords:** Ultra Wideband (UWB) Antenna, Rhombus-Shaped Antenna, Ground Penetrating Radar (GPR).

## 1 Introduction

ULTRA-WIDEBAND (UWB) signal is defined to be a signal that has a bandwidth of larger than 0.5 GHz and/or a fractional bandwidth superior than 20% [1]. The UWB has been officially allocated by the Federal Communications Commission (FCC) in 2002 to exploit an expansive bandwidth of 7.5 GHz expanding from 3.1 GHz to 10.6 GHz band. Within this band, a variety of UWB antennas have been proposed for different applications, such as surfaces penetrating and radar imaging [2-4]. Ground Penetrating Radar (GPR) is

a beneficial technique that exploits the electromagnetic waves for many applications such as the penetration of surfaces for the detection of objects hidden underneath. Nowadays, the variety of GPR applications require diverse GPR systems with various GPR antennas. GPR is considered as one of the UWB technology application by the employment of UWB antennas in GPR systems for the inspection of sub-surfaces where different penetration depths are needed. Besides, GPR technology could be useful for various media inspection [5-10]. There are several UWB antennas proposed for GPR systems but the majority of them are complex and/or costly like those proposed in [11-22]. Hence, there is constantly a necessity to design novel structures characterized by a high capability of penetration for different GPR systems. In this paper, we propose an easy-to-design, low-profile and low-cost compact CPW-fed Rhombus-shaped antenna for GPR applications. To enlarge the bandwidth, a change is included in the ground plane surrounding the radiating patch. All the simulations presented in this work are accomplished using the software CST Microwave Studio<sup>TM</sup> release [23]. The capability of penetration for the

Iranian Journal of Electrical and Electronic Engineering, 2021.  
Paper first received 28 November 2020, revised 27 February 2021, and accepted 06 March 2021.

\* The authors are with the Laboratoire des Télécommunications, Département d'Electronique et Télécommunications, Faculté des Sciences et de la Technologie, Université 8 Mai 1945 Guelma, BP 401, Guelma 24000, Algeria.

E-mails: [abdelhalim.chaabane@univ-guelma.dz](mailto:abdelhalim.chaabane@univ-guelma.dz) and [guerroui.mohammed@univ-guelma.dz](mailto:guerroui.mohammed@univ-guelma.dz).

Corresponding Author: A. Chaabane.  
<https://doi.org/10.22068/IJEEE.17.4.2041>

fabricated antenna has been verified throughout a mass of Concrete. An excellent capability of penetration is perceived that proves the utility of the antenna for GPR applications.

## 2 Antenna Design and Results

The detailed configuration and the dimensions of the designed antenna are shown in Fig. 1. The designed antenna is constructed by a Rhombus-shaped radiating patch and a modified ground plane. The antenna shape progression during the design steps is presented in the Fig. 2. We have started our design by a simple monopole antenna (antenna 1) that is composed by a radiating patch surrounded by the ground plane like in [24-26]. The patch, the feed line and the ground plane are printed on the same face of the substrate. In the second stage, a modification was introduced in the ground plane by eliminating the metal from the upper part of the ground plane (antenna 2). The aim of this cut was to affect the mutual coupling in the area between the patch and the ground plane by introducing an additional capacitive coupling. Additionally, the introduced cuts in the ground plane can minimize the weight of the antenna and reduce the conductor losses. In the final stage, a corrugation structure was applied along the edge of the ground plane below the patch (antenna 3) to more affect the capacitive coupling

between the ground plane and the patch. Consequently, the working bandwidth and the matching are greatly enhanced after introducing these modifications in the ground plane. The proposed antenna is designed with the use of an inexpensive 1.5-mm-thick FR4 epoxy substrate that has a relative dielectric of 4.4. The overall size of the antenna is only  $0.2721\lambda_0 \times 0.2093\lambda_0 \times 0.0157\lambda_0$  at 3.14 GHz. An expanded working bandwidth is attained by introducing modifications in the ground plane that affected the inductive and capacitive coupling in the area between the ground plane and the patch. A  $50 \Omega$  CPW transmission line is related to the Rhombus-shaped. The optimized dimensions of the proposed structure are as follows:  $L=26$  mm,  $L_1=4.5$  mm,  $L_2=4.71$  mm,  $L_3=8.5$  mm,  $L_4=3.06$  mm,  $L_5=3$  mm,  $R=0.5$  mm,  $a=4$  mm,  $W=20$  mm,  $W_1=8.5$  mm,  $W_2=2.5$  mm,  $W_3=1$  mm,  $W_4=4.6$  mm,  $W_5=5.6$  mm,  $b=7$  mm.

Fig. 3 illustrates that an extension of the operational bandwidth of about 4.636 GHz (45.75%) is achieved by eliminating the metal from the upper part of the ground plane (antenna 2). In addition, another extension of about 3.28 GHz (17.91%) is attained by using the corrugation structure on the ground plane (antenna 3). The operational bands and bandwidths of the three antennas are given in Table 1.

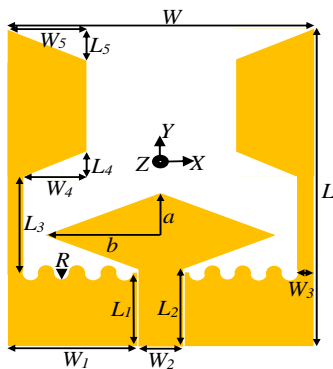


Fig. 1 Detailed configuration of the designed Rhombus-shaped antenna.

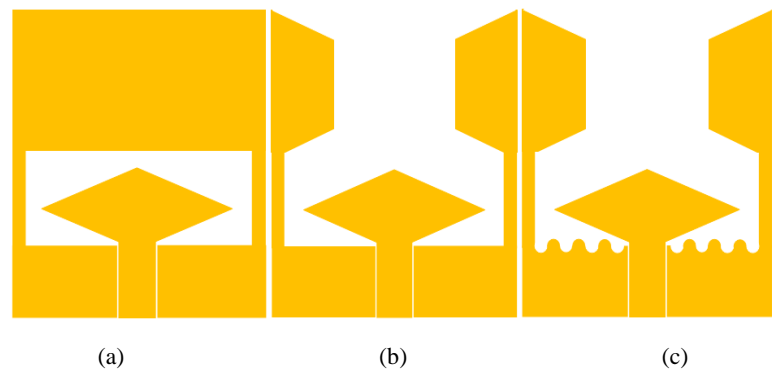


Fig. 2 Antenna design development, a) Antenna 1, b) Antenna 2, and c) Antenna 3.

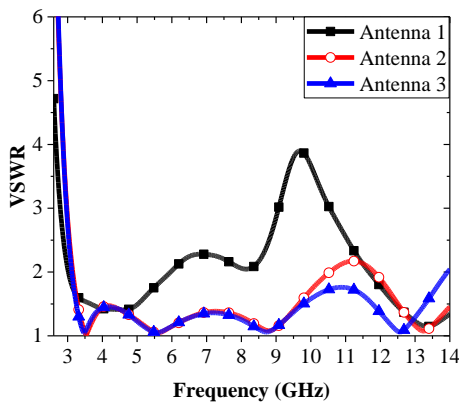


Fig. 3 Voltage standing wave ratio comparisons of the designed antenna with those of the primary designs.

Table 1 Antennas working bands and bandwidths (BW) comparisons.

Antennas	Working Band [GHz]	BW [GHz]	BW [%]
Antenna 1	3.056-5.82	2.764	62.28
Antenna 2	3.15-10.55	7.4	108.03
Antenna 3	3.14-13.82	10.68	125.94

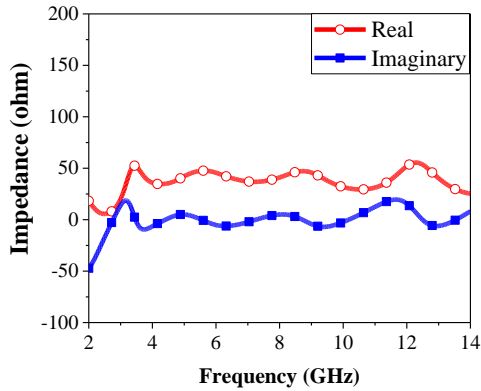


Fig. 4 Real and imaginary impedance.

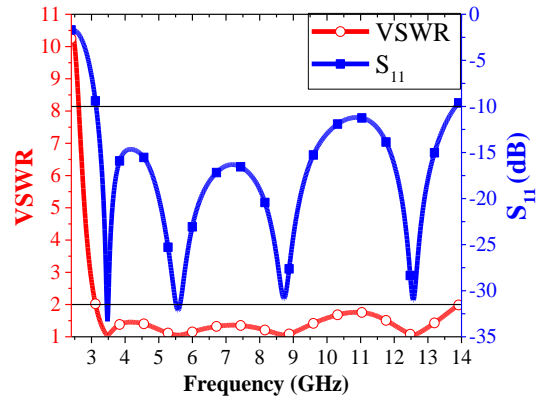


Fig. 5 Simulated VSWR and  $S_{11}$  of the proposed antenna.

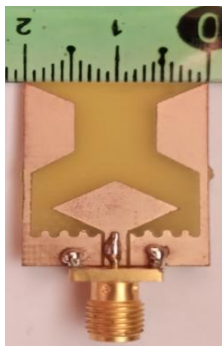


Fig. 6 Fabricated prototype.

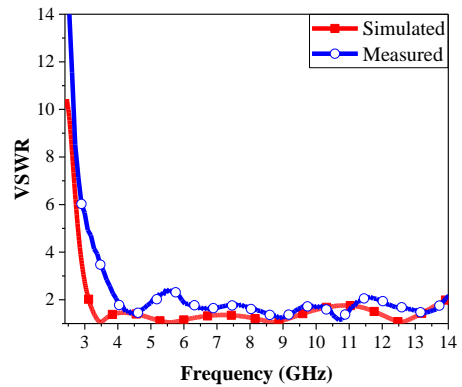
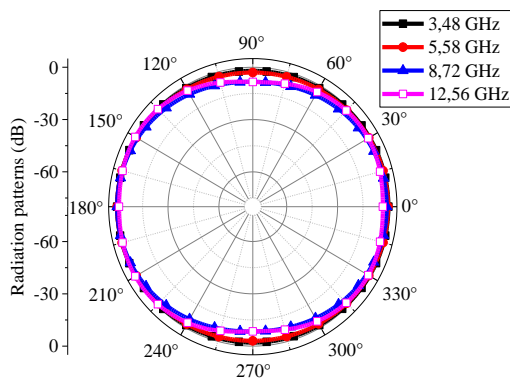
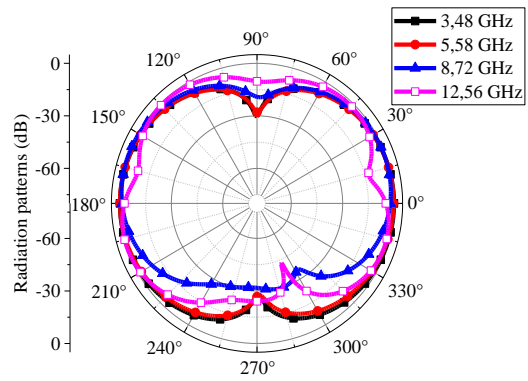


Fig. 7 Measured and simulated VSWR of the proposed antenna.



(a)



(b)

Fig. 8 Simulated radiation patterns at fourth frequencies; a)  $xz$ -plane and b)  $yz$ -plane.

Fig. 4 shows that the real part of the antenna impedance characteristic is nearly equal to 50 ohms value that is the impedance of the antenna port. While, the imaginary part is nearly oscillating around zero line which signifies the good adaptation of the designed antenna throughout the working band.

Fig. 5 depicts the calculated Voltage Standing Wave Ratio (VSWR) and the reflection coefficient ( $S_{11}$ ) of the antenna against the frequency. It is shown that the designed antenna works in a wide bandwidth ranging between 3.14 GHz and 13.82 GHz. The fabricated prototype is presented in Fig. 6. Fig. 7 shows that the

fabricated prototype is nearly operates between 3.95 GHz and 13.92 GHz. The small inconsistency between the simulated VSWR and the measured one may be attributed to the intolerance in the fabrication and measurement phases, losses in the port of the connection, and to unacceptable effects of the soldering.

The maximized far-field radiation patterns of the designed antenna is simulated in both the  $xz$ -plane (H-plane) and the  $yz$ -plane (E-plane) for fourth resonant frequencies from the operating band: 3.48 GHz, 5.58 GHz, 8.72 GHz, and 12.56 GHz. Fig. 8 shows that the designed antenna has excellent omnidirectional

patterns in the  $xz$ -plane and nearly bidirectional patterns in the  $yz$ -plane; comparable patterns are presented in [27]. Besides, the far-field radiation patterns undergo very feeble deformations in form at higher frequencies due to the excitation of higher order modes. Fig. 9 indicates that the values of the gain are almost varying between 1.1 dBi and 6.25 dBi which are superior than the values attained in [28]. Furthermore, higher radiation efficiency values of more than 80% are obtained in the considered band which are superior than those obtained in [29].

The evaluation of the pulse dispersion by calculating the group delay and the phase response of the transfer function ( $S_{21}$ ) is crucial in UWB antenna design especially for radar and imaging applications. For the simulations, two antennas were aligned face-to-face and separated by a distance of 0.3 m. The simulated group delay and the phase response of  $S_{21}$  are presented in the Fig. 10. A stable variation of the phase response of  $S_{21}$  with a variation of the group delay less than 0.5 ns are obtained within the working frequency range. The Non-varying responses of the group delay and of the phase response of  $S_{21}$  indicate the low dispersion which is suitable for GPR applications.

### 3 Ground Penetration Test

A solid masse of Concrete is placed in touch condition

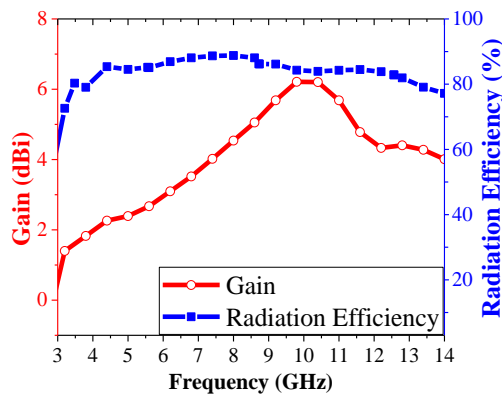


Fig. 9 Gain and radiation efficiency curves obtained by the designed antenna.

with the antenna to check the penetration capability for the antenna. A solid masse of Concrete with an average size of around  $160 \times 110 \times 69 \text{ mm}^3$  was fabricated. It was prepared by mixing water with the same fraction of: Grey Portland Cement Powder, White Building Sand, Yellow Building Sand, and Crushed Gravel. Measuring the antenna bandwidth in touch condition with the masse of Concrete is a powerful tool to ensure that the antenna is working with its stated specifications and so to verify the utility of the antenna for GPR applications. As presented in Fig. 11, the fabricated antenna was measured by keeping it in touch condition to the upper face of the fabricated masse for joining the electromagnetic energy into it. Hence, the antenna with the masse of Concrete are considered as a single device that is characterized by its specific characteristics and performances. As given in Fig. 12, an acceptable matching performance is obtained in the considered bandwidth for the antenna with the fabricated masse of Concrete indicating that almost the power provided to the antenna is transmitted which mean a good penetrating capability.

According to [30], the lower frequency of a printed monopole antenna is inversely proportional with its dimensions for these reasons a small difference is observed in lower frequency side (the dimensions of the antenna with Concrete is greater than the dimensions of

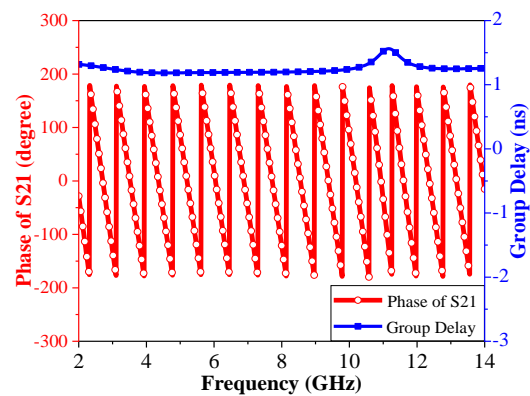


Fig. 10 Simulated group delay and phase response of  $S_{21}$ .

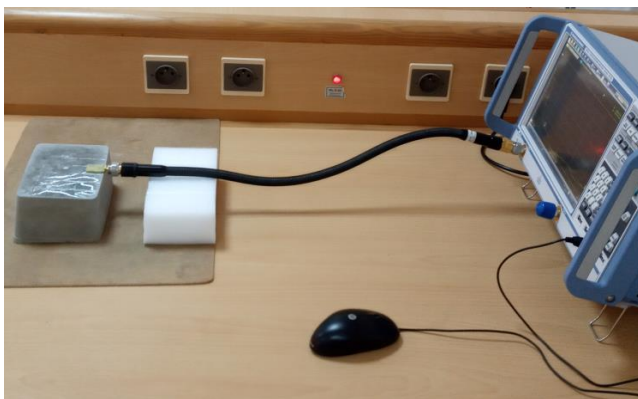


Fig. 11 GPR test setup.

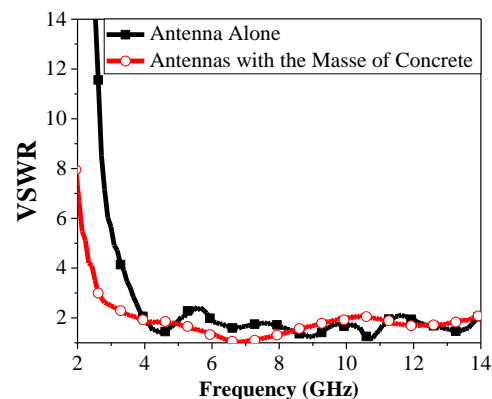


Fig. 12 VSWR measurements of the antenna alone and with the masse of Concrete.

**Table 2** Antenna parameters comparison with those of some others previously cited GPR antennas.

Ref.	Shapes	Structures	Sizes [mm <sup>3</sup> ]	Bandwidths [GHz]	Complexity/ease of fabrication
[11]	3D	Horn	410 × 300 × 800	1 – 2	Complex/costly
[12]	Multilayer	Bowtie	240 × 240 × 43.17	0.8 – 1.34	Complex/costly
[13]	Planer	Monopole	225 × 200 × 1.6	0.1 – 6	Simple/costly
[14]	Planer	Vivaldi	120 × 130 × 10	0.4 – 10	Complex/costly
[15]	Planer	Bowtie	107.7 × 68 × 0.8	0.98 – 4.5	Simple/costly
[16]	Multilayer	Monopole with reflectors	44 × 44 × 34	3 – 20	Complex/costly
[17]	Multilayer	Monopole with reflectors	44 × 44 × 20	3 – 14.64	Complex/costly
[18]	Planer	Monopole	220 × 180 × 1.6	0.6 – 4	Simple/costly
[19]	Planer	Bowtie	162 × 162 × 39	1 – 4	Complex/costly
[20]	3D	Horn	178 × 140 × 251	0.83–12.8	Complex/costly
[21]	3D	Horn	89.2 × 49.2 × 78.2	1.4–11	Complex/costly
[22]	Planer	Vivaldi	450 × 600 × 1.5	0.3 – 2	Simple/costly
This work	Planer	Monopole	26 × 20 × 1.5	3.14 – 13.82	Simple/low cost

the antenna alone). Despite the small shifting for VSWR at lower frequency side, the lower frequency edge for VSWR=2 is nearly the same for the antenna alone and with Concrete. Table 2 depicts a comparison of the proposed antenna with some formerly reported GPR antennas. As it is observed, the characteristics and the performances of our uncomplicated design are better or comparable to some other GPR antennas. Consequently, it could be concluded that our design can be very useful for GPR applications.

#### 4 Conclusion

We have proposed an easy-to-design, low-profile and inexpensive compact printed CPW-fed UWB Rhombus-shaped antenna for GPR applications. The operating bandwidth has been extended by introducing modifications in the ground plane surrounding the radiating patch. The calculated bandwidth broadens from 3.14 GHz to 13.82 GHz (125.94%) and the measured bandwidth extends nearly from 3.95 GHz to 13.92 GHz (111.58%). The working of the fabricated antenna is checked through a solid mass of Concrete to check its proficiency to work as a GPR antenna. Suitable results are persuaded that confirm the utility of the antenna for GPR applications.

#### Acknowledgement

This work was supported by the directorate general for scientific research and technological development (DG-RSDT) of Algeria.

#### References

- [1] M. A. Ahmed, H. M. Bahig, and H. Al-Mahdi, "Recent approaches to enhance the efficiency of ultra-wide band MAC protocols," *International Journal of Advanced Computer Science and Applications*, Vol. 8, No. 12, pp. 404–410, 2017.
- [2] D. Lee, G. Shaker, and W. Melek, "Investigation on the effects of resistive loading on wrapped bow-tie antennas," *International Journal of Microwave and Wireless Technologies*, Vol. 11, No.4, pp. 390–400, 2019.
- [3] A. Chaabane, O. Mahri, D. Aissaoui, and N. Guebgoub, "Multiband stepped antenna for wireless communication applications," *Informacije MIREM*, Vol. 50, No. 4, pp. 275–284, 2020.
- [4] D. Aissaoui, A. Chaabane, A. Boualleg, and M. Guerroui, "Coplanar waveguide-fed UWB slotted antenna with notched-band performance," *Periodica Polytechnica Electrical Engineering and Computer Science*, Vol. 65, No. 1, pp. 69–73, 2021.
- [5] C. Warren and A. Giannopoulos, "Characterisation of a ground penetrating radar antenna in lossless homogeneous and lossy heterogeneous environments," *Signal Processing*, Vol. 132, pp. 221–226, 2017.
- [6] M. D. O. F. Howlader and T. P. Sattar, "Miniaturization of dipole antenna for low frequency ground penetrating radar," *Progress in Electromagnetics Research C*, Vol. 61, pp. 161–170, 2016.
- [7] A. Chaabane and A. Babouri, "Dual band notched UWB MIMO antenna for surfaces penetrating application," *Advanced Electromagnetics*, Vol. 8, No. 3, pp. 6–15, 2019.
- [8] S. Kundu, "An ultra-wideband dual frequency notched circular monopole antenna for ground penetrating radar application," in *IEEE URSI Asia-Pacific Radio Science Conference (AP-RASC)*, New Delhi, India, pp. 1–4, 2019.
- [9] D. Seyfried, R. Jansen, and J. Schoebel, "Shielded loaded bowtie antenna incorporating the presence of paving structure for improved GPR pipe detection," *Journal of Applied Geophysics*, Vol. 111, pp. 289–298, 2014.

- [10] P. Cao, Y. Huang, and J. Zhang, "A UWB monopole antenna for GPR application," in *6<sup>th</sup> European Conference on Antennas and Propagation (EUCAP)*, Prague, Czech Republic, pp. 1837–1840, 2012.
- [11] A. H. Abdelgwad and T. M. Said, "L band horn antenna radiation enhancement for GPR applications by loading a wire medium," *Microwave and Optical Technology Letters*, Vol. 59, No. 10, pp. 2558–2563, 2017.
- [12] M. Elsaid, K. R. Mahmoud, M. Hussein, M. F. O. Hameed, A. Yahia, and S. S. A. Obayya, "Ultra-wideband circularly polarized crossed-dual-arm bowtie dipole antenna backed by an artificial magnetic conductor," *Microwave and Optical Technology Letters*, Vol. 61, No. 12, pp. 2801–2810, 2019.
- [13] A. Raza, W. Lin, Y. Liu, A. B. Sharif, Y. Chen, and C. Ma, "A magnetic-loop based monopole antenna for GPR applications," *Microwave and Optical Technology Letters*, Vol. 61, No. 4, pp. 1052–1057, 2019.
- [14] D. N. Elsheakh and E. A. Abdallah, "Compact ultra-wideband Vivaldi antenna for ground-penetrating radar detection applications," *Microwave and Optical Technology Letters*, Vol. 61, No. 5, pp. 1268–1277, 2019.
- [15] M. Joula, V. Rafiei, and S. Karamzadeh, "High gain UWB bow-tie antenna design for ground penetrating radar application," *Microwave and Optical Technology Letters*, Vol. 60, No. 10, pp. 2425–2429, 2018.
- [16] S. Kundu, "Experimental study of CPW-fed printed UWB antenna with radiation improvement for ground coupling GPR application," *Microwave and Optical Technology Letters*, Vol. 60, No. 10, pp. 2462–2467, 2018.
- [17] S. Kundu, A. Chatterjee, S. K. Jana, and S. K. Parui, "Gain enhancement of a printed leaf shaped UWB antenna using dual FSS layers and experimental study for ground coupling GPR applications," *Microwave and Optical Technology Letters*, Vol. 60, No. 6, pp. 1417–1423, 2018.
- [18] A. Raza, W. Lin, Y. Chen, Z. Yanting, H. T. Chattha, and A. B. Sharif, "Wideband tapered slot antenna for applications in ground penetrating radar," *Microwave and Optical Technology Letters*, Vol. 62, No. 7, pp. 2562–2568, 2020.
- [19] S. Liu, M. Li, H. Li, L. Yang, and X. Shi, "Cavity-backed bow-tie antenna with dielectric loading for ground-penetrating radar application," *IET Microwaves, Antennas & Propagation*, Vol. 14, No. 2, pp. 153–157, 2020.
- [20] J. Shao, G. Fang, J. Fan, Y. Ji, and H. Yin, "TEM horn antenna loaded with absorbing material for GPR applications," *IEEE Antennas and Wireless Propagation Letters*, Vol. 13, pp. 523–527, 2014.
- [21] D. Oloumi, P. Mousavi, M. I. Pettersson, and D. G. Elliott, "A modified TEM horn antenna customized for oil well monitoring applications," *IEEE Transactions on Antennas and Propagation*, Vol. 61, No. 12, pp. 5902–5909, 2013.
- [22] J. Guo, J. Tong, Q. Zhao, J. Jiao, J. Huo, and C. Ma, "An ultrawide band antipodal Vivaldi antenna for airborne GPR application," *IEEE Geoscience and Remote Sensing Letters*, Vol. 16, No. 10, pp. 1560–1564, 2019.
- [23] CST Microwave Studio, *Computer Simulation Technology (CST) version 2016*, Germany. Available at: <https://www.cst.com/Products/CSTMWS.2016>.
- [24] A. Sharma, P. Khanna, and A. Kumar, "A CPW-fed structure shaped substrate wideband microstrip antenna for wireless applications," *Journal of Microwaves, Optoelectronics and Electromagnetic Applications*, Vol. 16, No. 2, pp. 419–433, 2017.
- [25] M. D'Amico and F. M. Fasole, "Multi-trap CPW-fed wide slot antenna for UWB applications," in *6<sup>th</sup> European Conference on Antennas and Propagation (EUCAP)*, Prague, Czech Republic, pp. 1860–1864, 2011.
- [26] M. E. C. Gómez, H. F. Álvarez, B. P. Valcarce, C. G. González, J. Olenick, and F. L. H. Andrés, "Zirconia-based ultra-thin compact flexible CPW-fed slot antenna for IoT," *Sensors*, Vol. 19, No. 14, pp. 1–15, 2019.
- [27] D. Aissaoui, A. Chaabane, and A. Bouacha, "Compact super uwb elliptical antenna with corrugations for wireless communication systems," in *1<sup>st</sup> International Conference on Innovative Research in Applied Science, Engineering and Technology (IRASET)*, Meknes, Morocco, pp. 1–4, 2020.
- [28] M. M. Hosain, S. Kumari, and A. K. Tiwary, "Sunflower shaped fractal filtenna for WLAN and ARN application," *Microwave and Optical Technology Letters*, Vol. 62, No. 1, pp. 346–354, 2020.
- [29] T. Saeidi, I. Ismail, W. P. Wen, and A. R. H. Alhawari, "Ultra-wideband elliptical patch antenna for microwave imaging of wood," *International Journal of Microwave and Wireless Technologies*, Vol. 11, No. 9, pp. 948–966, 2019.

[30]K. P. Ray, "Design aspects of printed monopole antennas for ultra-wide band applications," *International Journal of Antennas and Propagation*, p. 713858, Vol. 2008, 2008.



**A. Chaabane** received his Ph.D. and completed his habilitation in Electronics in 2017 and 2020, respectively. He is currently working as an associate professor in the Université 8 Mai 1945 Guelma, Algeria. He is a member of Telecommunications Laboratory, Université 8 Mai 1945 Guelma. His main research interest includes fractal antennas,

ultra-wideband antennas, metamaterial antennas and GPR antennas.



**M. Guerroui** is currently a Ph.D. student in the Université 8 Mai 1945 Guelma, Algeria. He is a member of Telecommunications Laboratory, Université 8 Mai 1945 Guelma. His main research interest includes: fractal antennas, ultra-wideband antennas and GPR antennas.



© 2021 by the authors. Licensee IUST, Tehran, Iran. This article is an open access article distributed under the terms and conditions of the Creative Commons Attribution-NonCommercial 4.0 International (CC BY-NC 4.0) license (<https://creativecommons.org/licenses/by-nc/4.0/>).